Fibers and Polymers 2017, Vol.18, No.8, 1623-1628
DOI 10.1007/s12221-017-1157-y

ISSN 1229-9197 (print version)
ISSN 1875-0052 (electronic version)

A Hyperelastic Approach for Finite Element Modelling Puncture Resistance of Needle Punched Nonwoven Geotextiles

Elnaz Saberi[1]*, Saeed Shaikhzadeh Najar[1], Sayyed Behzad Abdellahi[2], and Zeynab Soltanzadeh[1]

[1]*Department of Textile Engineering, Amirkabir University of Technology, Tehran 159163-4311, Iran*
[2]*Department of Textile Engineering, Isfahan University of Technology, Isfahan 84156-8311, Iran*
(Received November 29, 2016; Revised April 23, 2017; Accepted May 29, 2017)

Abstract: Needle-punched nonwoven fabrics are the most common textile structures used as geotextiles. In most applications, geotextile layers are subjected to compressive forces perpendicular to their plane. These forces will lead to the deformation of the layers and eventually cause puncture. In this study, the puncture behavior of nonwoven fabrics was simulated based on hyperelastic model, using finite element method (FEM) and considering geotextile layer as a continuous surface. For this purpose, three needle-punched fabrics with different weights of 460, 715, and 970 gr/m^2 were selected and two tests of CBR (ASTM D6241) and Pin (ASTM D4833) were considered to evaluate the puncture process. Thus, puncture behavior of fabrics based on both of these tests were simulated using the ABAQUS software. Considering the puncture behavior in terms of stress-strain diagrams, results obtained from experiments and finite element analysis (FEA), showed good agreement. It was also shown that non-woven fabrics with higher weight exhibited higher puncture stress in both CBR and Pin tests. The mechanism of puncture at macroscopic scale obtained by finite element method was also qualitatively compared to that of experimental results.

Keywords: Puncture resistance, Finite element analysis, Hyperelastic material model, Needle punched nonwoven geotextile, Pin and CBR tests

Introduction

Needle punched nonwoven fabrics are the most commonly used textile structures as geotextiles for performing reinforcement, filtration, drainage and separation functions. In most usages, the geotextiles are subjected to concentrated forces perpendicular to its plane while the fabric is under in-plane tensions due to subgrade surface irregularities [1]. Thus, the ability of geotextiles to withstand stresses imposed perpendicularly to fabric surface can be evaluated through puncture resistance testing. Pin puncture strength and CBR puncture strength are two well-known standard test methods to evaluate puncture behavior.

There are several research studies investigating the puncture resistance of geotextile fabrics. Rawal *et al*. [1] studied the effect of process parameters including web area density, punch density, and depth of needle penetration on puncture resistance in the machine and cross-machine directions properties of needle punched nonwoven geotextiles. Li *et al.* [2] evaluation high-modulus, puncture-resistant composite nonwoven fabrics via response surface methodology. Their results showed that static puncture resistance strength has linear dependence on bursting strength. Ghosh [3] studied puncture resistance of geotextiles under uniform radial pre-strain. Their test results show lower failure strain in punctures if the test sample is pre-strained. The failure strain measured in wide width tensile tests are much higher than calculated strains in punctures. Bergardo [4] studied the effect of axisymmetric loading, puncture speed and fabric weight on the loading capacity of soil-geotextile system with different types of geotextile. The calculated results indicate an additional load capacity due to the presence of the geotextile using an axisymmetric stiffness which demonstrated a significant contribution of membrane action by the different types of geotextile on the increase in bearing capacity of soil-geotextile system. Koerners [5] studied the puncture resistance of PET and PP needle punched nonwoven geotextiles using three different probe shape types. Recently, Askari *et al.* [6] studied the effects of both test speed and fabric weight on the puncture resistance of polyester needle punched nonwoven fabrics. There are several research studies that have investigated the puncture resistance of other fabrics. Hassim *et al.* [7] studied puncture resistance of natural rubber latex unidirectional coated fabrics. Lin *et al.* [8] studied puncture-resisting on polypropylene-selvages reinforced composite nonwovens. The results show that, polypropylene nonwoven selvages improved static puncture resistance.

On the other hand, the use of finite element software to study puncture mechanism is developed in recent years.

Yahya *et al*. [9] studied effect of impactor shapes and yarn frictional effects on plain woven fabric puncture with simulation. Their results showed that puncture damage behavior is the critical dependent of the magnitude of impactor shapes and yarn frictional contacts. Sun *et al*. [10] investigated of puncture behaviors of woven fabrics from finite element analyses (FEA) and experimental tests. From their FEA results, they found that the puncture damage includes three stages: fabric tension, weft and warp yarn slippage, and yarn breakage and pullout. In addition, nonlinear elastic model in some research has been use to simulation

*Corresponding author: e.saberi@aut.ac.ir

mechanical behavior of textile materials [11-13]. Yoo and Kim [14] use hyperelastic model to simulation mechanical behavior of geosynthetic reinforced segmental retaining wall. In an extensive study, Abdellahi *et al*. [15] simulation flexural behavior of textile reinforced concrete which used geotextile fabric in structure of samples. They use hyperelastic material to simulation mechanical behavior of geotextile.

This study is in conjunction with previous research work of the author (Askari *et al.* [6]) and aimed to model and simulate the puncture resistance of needle punched nonwoven geotextiles using a developed hyperelastic finite element model.

Experimental

Maeterials

In this study, three nonwoven fabrics with different weights (460, 715, 970 gr/m^2) were selected. All of geotextile fabrics were manufactured by needle punched process. The properties of nonwoven samples that are used to tests and simulate the behavior of puncture are given in Table 1.

Test Methods

In order to investigate the puncture behavior of the geotextiles, CBR and Pin tests were conducted. CBR, which stands for California Bearing Ratio, is a test for measuring geosynthetics puncture resistance. The CBR test was conducted according to ASTM D6241 [16]. A clamp and a cylindrical plunger were designed and constructed. The clamp consisted of two circular plates with inner diameters of 150 mm. The geotextile specimen was held and secured between theses plates by eight screws. The cylindrical plunger diameter was 50 mm with a flat end. The plunger edge was a bit round with a radius of 2.5±0.5 mm. The plunger and the clamp were installed on a Zwick Universal Testing Machine which ran at a constant rate of elongation (CRE). The clamp was put beneath the plunger and centered. Tests were carried out with different speeds, 25, 50, 75, 100 and 125 mm/min, while the standard test speed was 50 mm/min. Then the plunger came down and punched the specimen secured in the clamp.

The Pin test was also carried out according to ASTM D4833 [17]. The procedure of this test was the same as the CBR test, but there were some differences. Here the clamp consisted of two circular plates with inner diameters of 45±0.25 mm. The indenter was smaller and its shape was different. The indenter diameter was 8±1 mm, having a flat end with a 45 ^{o} (0.8 mm) chamfered edge that contacted the specimen surface.

The geotextile specimen was held and secured between these plates by six screws. Then the indenter and the clamp were installed on the Zwick Universal Testing Machine, and ran at a constant rate of elongation, as was mentioned before.

A summary of the standards is shown in Table 2. Figures 1 and 2 show the testing fixtures and plungers used in this study.

Table 1. Specifications of the nonwoven fabric

Sample	Weight* (gr/m^2)	Thickness* (mm)	Density* (g/cm^3)
A	460	3.22	1.43
B	715	4.5	1.59
C	970	5.07	1.91

*Average value.

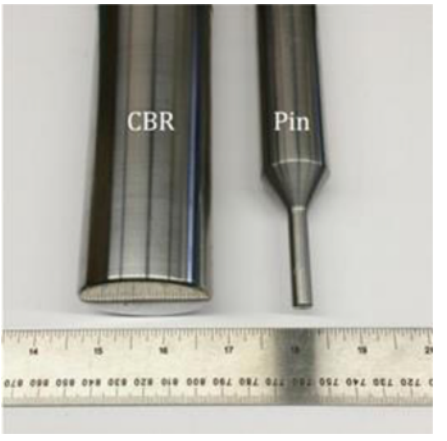

Figure 1. Plungers used for CBR and Pin puncture strength testing of geotextiles.

Table 2. Comparison of pin and CBR testing standards [7,8]

Measure	D4833 (Pin)	D6241 (CBR)
Probe diameter	8 mm±0.1 mm	50 mm±1 mm
Probe chamfer/edge	45 ^{o}, 0.8 mm	2.5 mm±0.5 mm
Specimen minimum outer diameter	100 mm	Clamp outer dia. + 10 mm
Specimen unsupported diameter (clamp inner diameter)	45 mm±0.025 mm	150 mm
Compression speed	300 mm±10 mm/min	50 mm/min
Maximum allowable slippage	None allowed	5 mm
Test conclusion	Break	Break
Resistance reported	Maximum	Maximum

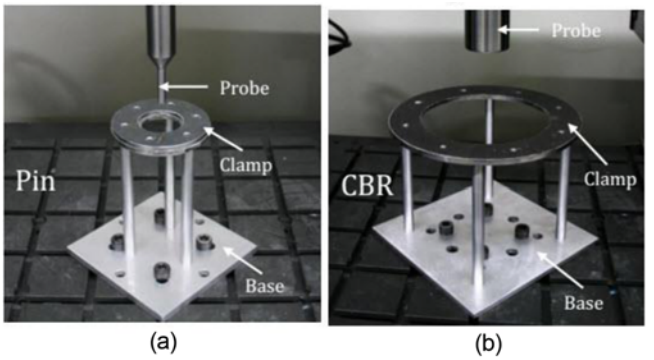

Figure 2. Clamping fixtures used for puncture strength testing of geotextiles; (a) Pin puncture fixture and (b) CBR fixture.

Table 3. Ogden model's coefficients for three fabric samples

Sample	μ_i	α_i	D_i
A	0.2125	5.4462	2.0161
B	0.3903	4.1497	1.0979
C	0.5788	4.4523	0.7404

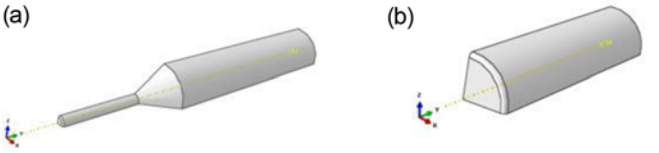

Figure 3. Geometrical model of the plunger puncture; (a) Pin plunger and (b) CBR plunger.

Finite Element Modeling

The finite element modeling was carried out based on the finite element software package ABAQUS (version 6.12).

Mechanical Behavior

Geotextile fabric classified as polymer materials, therefore their mechanical behavior should be considered as hyperelastic materials. A material model normally used to describe a geotextile response to loading is the non-linear hyperelastic model described by the Ogden strain energy formulation equation (1) [18]:

$$W(\lambda_1,\lambda_2,\lambda_3)=\sum_{i=1}^{N}\frac{2\mu_i}{\alpha_i^2}(\bar{\lambda}_1^{\alpha_i}+\bar{\lambda}_2^{\alpha_i}+\bar{\lambda}_3^{\alpha_i}-3)+\sum_{i=1}^{N}\frac{1}{D_i}(J^{el}-1)^{2i} \quad (1)$$

where N is a polynomial order, μ_i, α_i and D_i are temperature dependent parameters. λ_i are the principal extension ratios, $\bar{\lambda}_i$ as shown in the following equation (2):

$$\bar{\lambda}_i=J^{-1/3}\lambda_i \quad (2)$$

The coefficients μ_i, are related to the initial shear modulus μ_0, by the expression shown in the following equation (3):

$$\mu_0=\sum_{i=1}^{N}\mu_i \quad (3)$$

While the initial bulk modulus K_0, following equation (4):

$$K_0=\frac{2}{D_i} \quad (4)$$

The coefficients used in the hyperelastic model within ABAQUS can be defined directly, or alternatively, actual test data can be specified. Therefore the uniaxial, Pin and CBR test data have been used to predict mechanical behavior of fabric. The stress/strain data which were extracted from uniaxial, Pin and CBR tests imported to ABAQUS software and software started to calculate Ogden coefficients. ABAQUS uses curve fitting method to calculate Ogden coefficients. Table 3 shows Ogden model's coefficients for one strain energy potential order:

The finite element (FE) modeling was carried out based on the finite element software package ABAQUS/Explicit. The whole FE modeling includes the steel puncture and the circular nonwoven fabric specimen. Due to symmetry of the circular fabrics in puncture test, a quarter circular fabric sample could be selected to create the FE model. At the same time, a quarter part of the steel puncture could be employed in the FE model accordingly. Maximum stress damage was used to show puncture in fabric. When the stress of a single element reached the peak stress, the damage will be occurred. The geometrical models of a quarter plunger in the CBR and Pin test are shown in Figure 3. In experimental test, the plunger moved downwards and the fabric was fixed by holders. In FE model, the plunger moved downward at a speed of 50 and 300 mm/min in order to accomplish CBR and Pin tests respectively and the fabric was fixed. Surface to surface model was used to indicate components friction. The contact formulation between the specimens and loading instrument was hard contact in the normal direction, which gives strict enforcement of contact constraints.

Boundary Conditions

For maximizing computational efficiency, plungers were defined as rigid body in ABAQUS. The advantage of rigid body against deformable body is that rigid body analysis performed at the reference point with a maximum of six degrees of freedom [19]. On the other hand, deformable body with many degrees of freedom will result in extensive analysis time. In this study for initial conditions all degrees of freedom of the holders and plunger are closed. The fabric is constrained by holders. Tie constraint was used to hold the fabric by clamps. For this purpose, clamps surfaces were selected as master and fabric surface was selected as a slave surface in finite element software. In the next step a load is submitted to plunger by displacement in plunger axis direction. The plunger starts to move downwards until fabric fracture

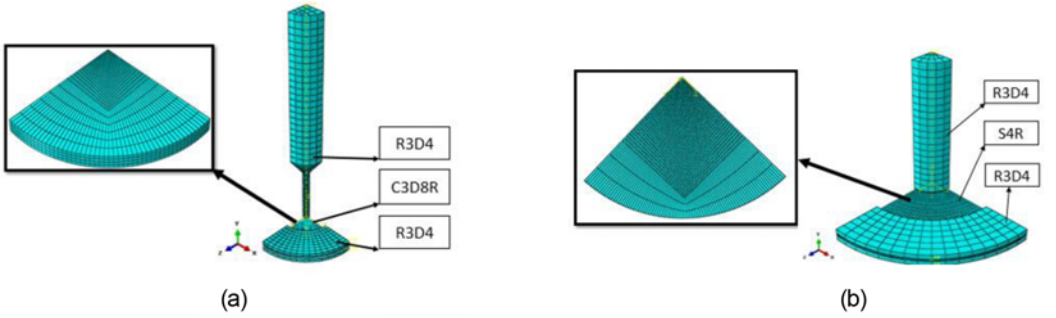

Figure 4. Mesh generation; (a) Pin test and (b) CBR test.

occurs as defined in the experimental program.

Mesh Generation

As shown in Figure 4, the probe and clamp were meshed with R3D4 shell element. The nonwoven was meshed for CBR and Pin tests with S4R and C38DR elements respectively. As obvious in Figure 2(a), in Pin test diameter to length ratio of fabric was low, therefore, the geotextile fabric was modeled as a solid mass. So, continuum elements were chosen to mesh generation of fabric in Pin test. The plunger and holders were selected as rigid body.

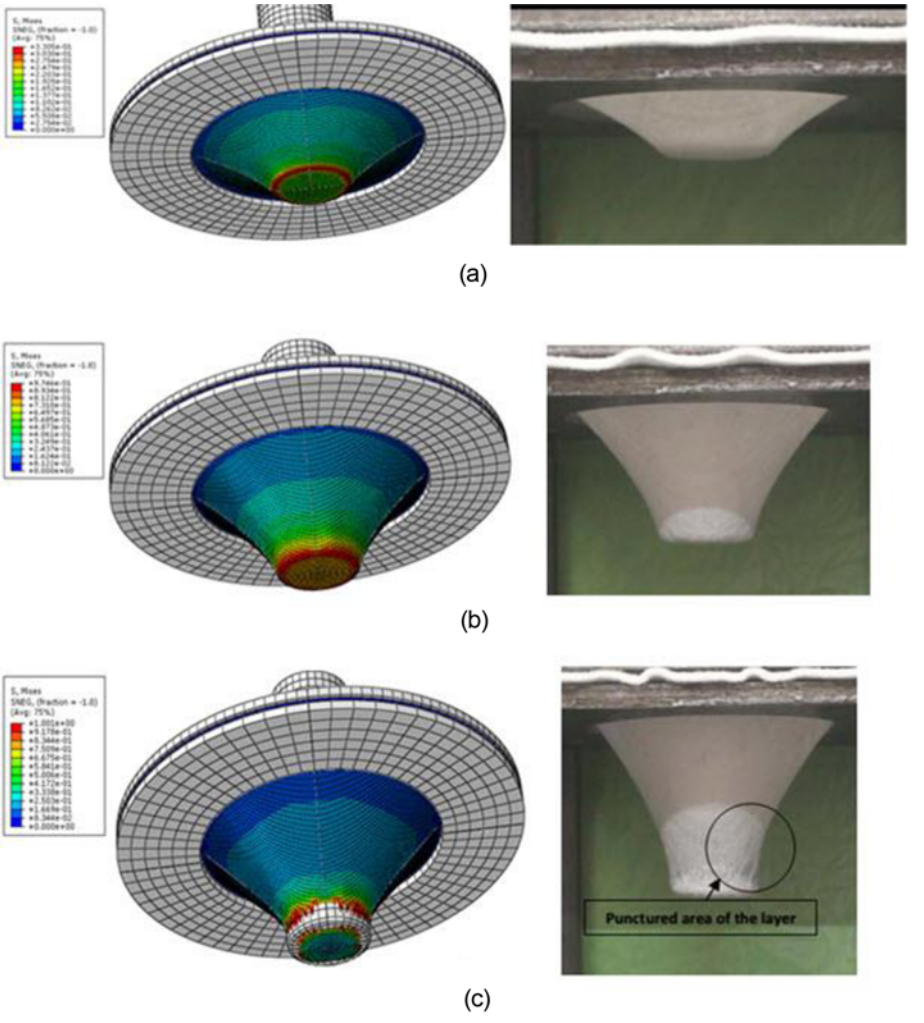

Figure 5. FEM and experimental results of puncture process of the nonwoven fabric for CBR test; (a) initial load, (b) fabric elongation, and (c) fabric fracture.

Results and Discussion

Figure 5 shows puncture steps of nonwoven fabric in FEA and experiments done for the CBR test. At the start of the test, the plunger began to come down, while the spaces between the fibers were empty, and the compression and tensional forces resulted in the movement of the fibers, so the fibers displayed a low resistance to those forces. In Figure 5 the fibers were tightly packed together, so they would be in complete contact with each other while the frictional forces increased. Thus, the fibers were locked and not easily moved. This situation is called Self-Locking mechanism. By continuing the downward movement of the plunger, the tension of the system rose, which resulted in the frictional forces moving the fibers. Understandably, the specimen showed the fibers in their new arrangement. In Figure 5(a), the plunger was just in contact with the specimen surface. In Figure 5(b), plunger move down and Self-Locking is occurred between fibers. In Figure 5(c), the puncture of the layer has occurred. In this region, the fibers were stuck and could not move, so the frictional forces suddenly separated the fibers and punching occurred.

Figure 6 shows the comparison of stress-strain curves between experimental and FEA results in CBR and Pin Tests. As it is obvious in Figure 6, there is an approximate agreement between FE simulation and the experimental

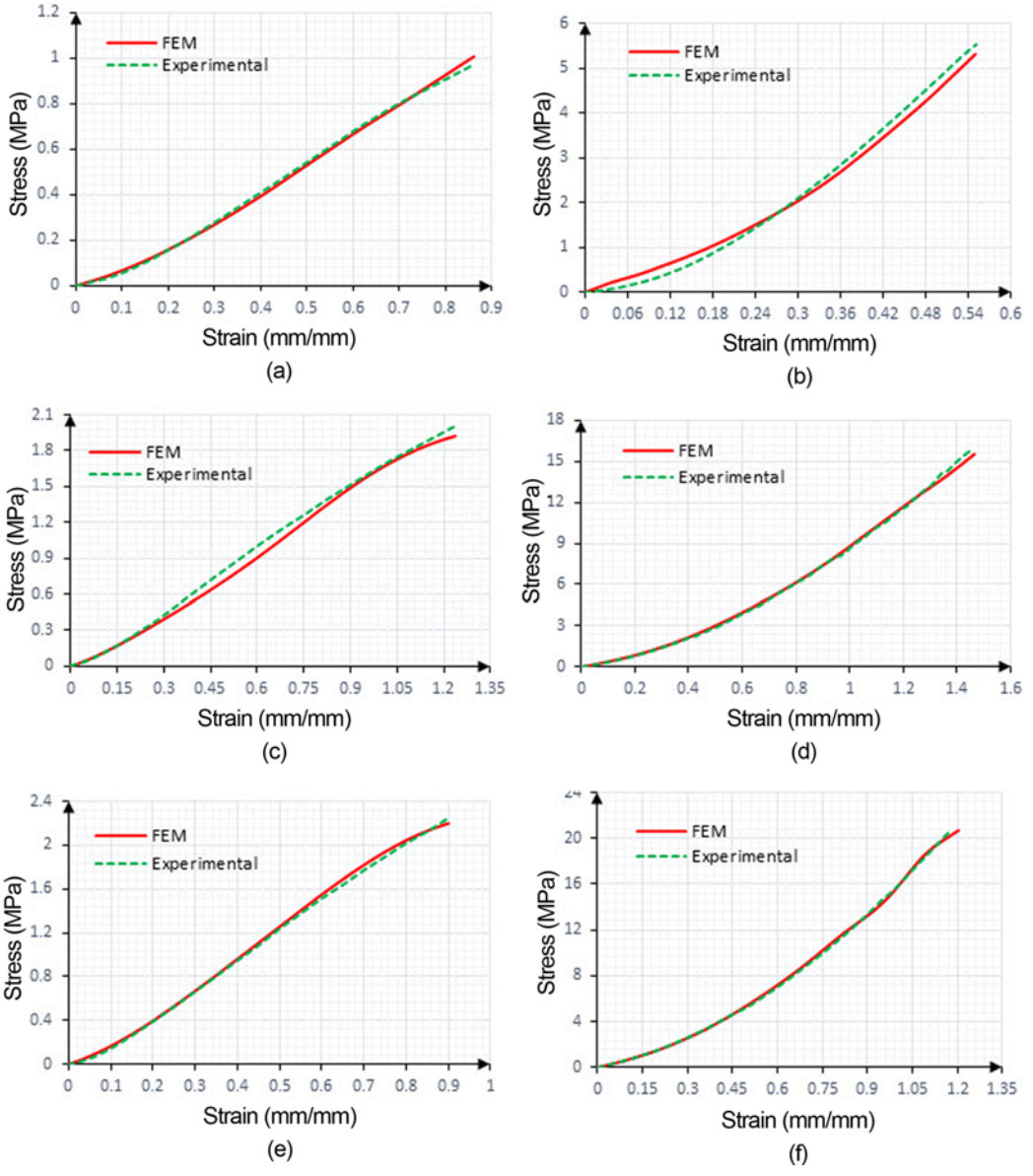

Figure 6. Comparisons of stress-strain curves between experiments and FEM; (a) CBR, 460 gr/m^2, (b) CBR, 715 gr/m^2, (c) CBR, 970 gr/m^2, (d) Pin, 460 gr/m^2, (e) Pin, 715 gr/m^2, and (f) Pin, 970 gr/m^2.

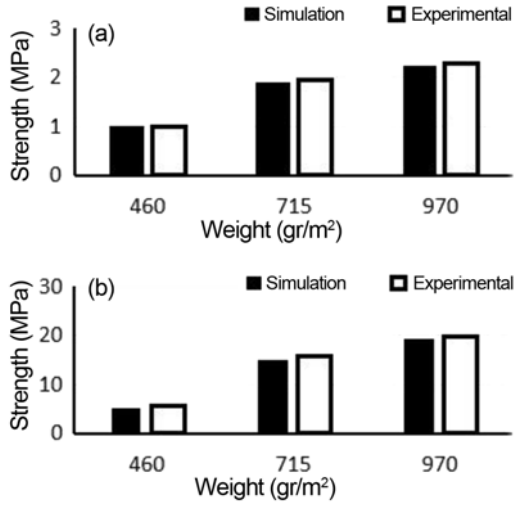

Figure 7. Comparisons of strength-weight curves; (a) CBR and (b) Pin.

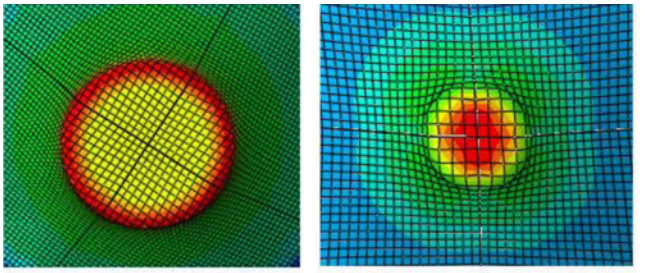

Figure 8. Interaction between nonwoven fabrics with the plunger; (a) CBR test and (b) Pin test.

results. The Ogden model for hyperelastic materials is also a suitable model for simulating nonwoven fabrics.

By increasing fabric weight more fiber amount get involve together and to puncture the fabric should be applied more load which can divided fibers. Therefore, the strength of geotextile fabric in CBR and Pin tests is increased by increasing geotextile fabric weight (Figure 7). Pin test bar diameter is smaller than CBR test bar diameter, thus maximum puncture resistance is reported for the Pin tests.

Figure 8(a) shows high "stress-ring" formation around the contact region of the CBR plunger surface with yarns. In contrast, the Pin plunger reported a higher stress formation region at the center fabric, as shown in Figure 8(b).

Using hyperelastic model for indicating mechanical behavior of the nonwoven fabric leads to change mechanical behavior of fabric from linear to nonlinear. These variations cause better correlation between experimental and numerical results. On the other hand, modeling a quarter components for fabric fracture simulating reduces solving time. But this method can't show fibers interactions and fibers deformation in micro scale.

Conclusion

This present study considers using finite element method to study the puncture behavior of a nonwoven fabric in macro-scale based on the hyperelastic model. Ogden model for hyperelastic materials has been used to simulate the mechanical behavior of nonwoven fabrics. CBR and Pin tests were simulated in ABAQUS finite element software according to standards. Considering the puncture behavior in terms of stress-strain diagrams, results obtained from experiments and FEA, showed good agreement. It was also shown that nonwoven fabrics with higher weight exhibited higher puncture stress in both CBR and Pin tests. The mechanism of puncture obtained by finite element method at macroscopic scale was also qualitatively compared to that of experimental results.

References

1. A. Rawal, S. Anand, and T. Shah, *J. Ind. Text.*, **37**, 341 (2008).
2. T.-T. Li, R. Wang, C. W. Lou, and J.-H. Lin, *J. Ind. Text.*, **43**, 247 (2013).
3. T. K. Ghosh, *Geotext. Geomem.* **16**, 293 (1998).
4. D. Bergado, S. Youwai, C. Hai, and P. Voottipruex, *Geotext. Geomem.*, **19**, 299 (2001).
5. G. R. Koerner and R. M. Koerner, *Geotext. Geomem.*, **29**, 360 (2011).
6. A. S. Askari, S. S. Najar, and Y. A. Vaghasloo, *J. Eng. Fiber. Fabric.*, **7**, 3 (2012).
7. N. Hassim, M. R. Ahmad, W. Y. W. Ahmad, A. Samsuri, and M. H. M. Yahya, *J. Ind. Text.*, **42**, 118 (2012).
8. J.-H. Lin, T.-T. Li, and C.-W. Lou, *J. Ind. Text.*, **45**, 1477 (2016).
9. M. F. Yahya, S. A. Ghani, and J. Salleh, *Text. Res. J.*, **84**, 1095 (2014).
10. B. Sun, Y. Wang, P. Wang, H. Hu, and B. Gu, *Text. Res. J.*, **81**, 992 (2011).
11. S. B. Abdellahi, E. Naghashzargar, and D. Semnani, *J. Ind. Text.*, doi:10.177/1528083716648762 (2016).
12. A. Charmetant, J. G. Orliac, E. Vidal-Sallé, and P. Boisse, *Compos. Sci. Technol.*, **72**, 1352 (2012).
13. A. Charmetant, E. Vidal-Sallé, and P. Boisse, *Compos. Sci. Technol.*, **71**, 1623 (2011).
14. C. Yoo and S.-B. Kim, *Geotext. Geomem.*, **26**, 460 (2008).
15. S. B. Abdellahi, S. M. Hejazi, and H. Hasani, *J. Sand. Stru. Mat.*, 1099636216665300 (2016).
16. ASTM D 6241-2009, ASTM International, West Conshohocken PA, 2009.
17. ASTM D 4833-2014, ASTM International, West Conshohocken PA, 2014.
18. R. W. Ogden, "Non-linear Elastic Deformations", Courier Corporation, 1997.
19. Simulia, "Abaqus/CAE User's Manual", USA, 2012.